JOURNAL OF CATALYSIS 131, 204–214 (1991)

Dual Mechanism of Pyridine Hydrodenitrogenation on MoS_x-Based Catalysts: Experimental Evidence

A. KHERBECHE, R. HUBAUT, J. P. BONNELLE, AND J. GRIMBLOT[1]

Laboratoire de Catalyse Hétérogène et Homogène, UA CNRS No. 04020, Université des Sciences et Techniques de Lille Flandres-Artois, 59655 Villeneuve D'Ascq Cedex, France

Received October 4, 1990; revised March 28, 1991

Hydrodenitrogenation (HDN) of pyridine has been performed on Mo and Ni–Mo-based catalysts first sulfided and then treated under H_2 at various temperatures T_R in order to progressively create anionic vacancies at the active phase. No H_2S has been admitted in the feed during the test performed at 3 MPa. The changes in the products and the effect of the H_2 partial pressure have been interpreted by a dual mechanism of HDN. The classical consecutive scheme to pentane as product with detection in the gas phase of piperidine as an intermediate product has been found dominent at low T_R. At higher T_R, with a more sulfur-deficient catalyst, another route without any detection of the intermediate piperidine has been observed. © 1991 Academic Press, Inc.

INTRODUCTION

Hydrodesulfurization (HDS) and hydrodenitrogenation (HDN), the necessary catalytic operations for cleaning petroleum fractions, are generally conducted on supported MoS_2-based catalysts associated with a promoter such as Co or Ni. These reactions are usually performed at temperatures higher than 350°C under high hydrogen pressure (typically ~100 atm). A detailed investigation of HDS and HDN reactions of natural cuts originating from crude oil does not permit precise elucidation of the mechanism of the reactions and the nature of the catalytic sites involved so that, in academic laboratories, those reactions are performed with model molecules such as thiophene, benzo- or dibenzothiophene, pyridine, quinoline, or acridine. Mechanisms and kinetics of the HDS reaction with such sulfur-containing molecules are relatively well documented (*1–3*). Concerning HDN, review articles (*3–6*) and early investigations by Satterfield and co-workers (*7–8*) or by McIlvried (*9*) permitted reaction networks to be established after identification of intermediate products when model N-containing molecules are used. For example, the following scheme proposed for pyridine HDN, the reaction of interest in this work, has been described by McIlvried (*9*):

Pyridine → piperidine →

n-pentylamine → pentane + NH_3.

The rate-determining step is generally assumed to be the piperidine transformation into *n*-pentylamine, but it may depend on the experimental conditions. Moreau *et al.* (*10*) showed that the HDN activity is related to the structure of model compounds from experiments performed over sulfided Ni–Mo- or Ni–W-supported catalysts in a batch reactor. They found that the saturation of the heteroaromatic ring always occurs prior to any C–N bond cleavage; the rate of hydrogenation of that ring is mostly influenced by its aromaticity. On the other hand, the basicity of nitrogen has an appreciable effect on the $C(sp^3)$–N bond hydrogenolysis. Laine (*11*) and Ledoux *et al.* (*12*) also suggested mechanistic explanations. In studying quinoline HDN, Laine (*11*) proposed homogeneous catalyst systems that

[1] To whom correspondence should be addressed.

0021-9517/91 $3.00

can model the reaction occurring on heterogeneous catalysts. The mechanistic elements supported by the work of Ledoux *et al.* (*12*) are perhaps not relevant to the practical HDN conditions as the MoO_3–Al_2O_3 catalyst they used was only reduced (the sulfidation step was omitted) and also because the experiments were carried out only at H_2 atmospheric pressure. Similar considerations on the chemical state of the catalyst can also be made regarding the study of pyridine hydrogenolysis over MoO_3-based catalysts by Sonnemans *et al.* (*13*). Indeed, in practical tests, there is H_2S present during the HDN reaction as the sulfur-containing molecules, always present, are more easily transformed (desulfurized) than the N-containing molecules. Therefore, more relevant are the studies of the HDN reaction on MoS_2-based catalysts with emphasis on the competition between HDS and HDN or on the effect of the presence of H_2S during HDN tests with N-containing aromatic probe molecules (*14, 15*). However, in that case, it is difficult to have a precise description of the working sites located at the MoS_2 active phase, as the simultaneous presence of H_2 and H_2S may influence the S/Mo stoichiometry of MoS_2. The alternative approach we propose in this study is to follow HDN of pyridine on MoS_2-based catalysts treated, before the catalytic tests, with pure H_2 at a given temperature (T_R) in order to create sulfur vacancies, the amount of which depends on T_R. No H_2S is used during the test so that the catalyst state depends only on T_R and not on the HDN conditions. Indeed, such a procedure has been applied with success to study hydrogenation and/or isomerization of dienes (isoprene, *cis*-, or *trans*-1-3 pentadiene), hydrogenation of toluene and HDN of pyridine (*16–18*). The aim of the present work is to present the changes in the mechanism of pyridine HDN when T_R is increasing.

EXPERIMENTAL

Two catalysts were studied, namely a 14 wt% MoO_3/Al_2O_3 and a 3 wt% NiO–14 wt% MoO_3/Al_2O_3 prepared according to the usual procedures. Pyridine (Fluka-Purissim > 99.8%) HDN was performed in a high-pressure catalytic flow microreactor. The catalysts were sulfided at 623 K and atmospheric pressure with 33 vol% of dimethyl disulfide in *n*-heptane. The catalyst was then treated with H_2 at different temperatures T_R to progressively remove labile sulfur and create anionic vacancies prior to being tested. The HDN reaction was performed with a sulfur-free feed at 3 MPa and 573 K with a ratio $H_2/HC = 75$ (and LHSV = 2). The products were analyzed by gas chromatography utilizing, respectively, a heated on-line gas sample valve, flame ionization detector, column packings of Carbowax-glass (for the nitrogen compounds), and SE 30 stainless steal (for hydrocarbons). Products were identified by comparison with pure samples. On a correctly sulfided catalyst, only piperidine, *n*-pentylamine, and pentane are generally obtained. On oxide or badly sulfided catalysts, many other products can be observed, such as cracked hydrocarbons, C_{10} hydrocarbons, *N*-pentylpiperidine, and other compounds (*12, 13, 19*). We have never observed more than 1% of *N*-pentylpiperidine. The fact that the solvent (*n*-heptane) does not give rise to hydrogenolysis by-products is a good test of a correctly sulfided state of the catalysts. Moreover, the use of *n*-heptane as an internal sample permits one to check the mass balance of reactants and products. Activities were calculated by considering the number of molecules converted or produced by unit mass of catalyst and time. Classically the space time W/F_i was defined by the ratio between the mass of catalyst W (in g) over the nitrogen compound (i) feed rate F_i (in mol of $i \times h^{-1}$). Selectivity into pentane (S_p in percentage) was given by the ratio of the amount of formed pentane over the amount of transformed pyridine.

RESULTS

Effects of the H_2 Pretreatment

In Fig. 1 are reported the molar distributions of the reactive compound (pyridine) and of the products (piperidine and pentane)

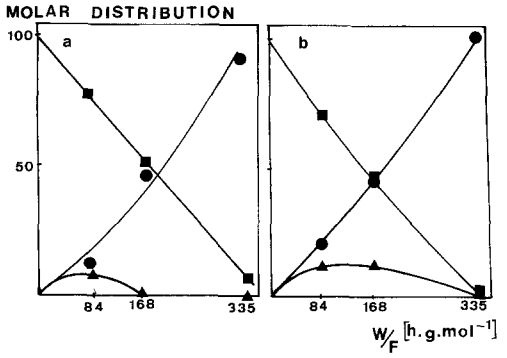

FIG. 1. Molar distribution of pyridine (■), piperidine (▲), and pentane (●) during pyridine HDN after pretreatment under H_2 at T_R = 623 K. (a) Mo/γ-Al_2O_3, (b) NiMo/γ-Al_2O_3.

as a function of the space time W/F_{pyridine} for a given T_R (623 K) on both the Mo and Ni–Mo catalysts. As the initial slope of the curve corresponding to piperidine formation is never equal to zero, it is inferred that this molecule is a primary product. This is in agreement with the reaction scheme proposed by McIlvried (*9*) in which pyridine is hydrogenated first into piperidine and before hydrogenolysis of the C–N bonds. Concerning the formation of pentane, its initial rate, sometimes smaller than that of piperidine formation, is never equal to zero. Therefore pentane can also be considered, at least for a fraction of it, as a primary product.

Within our working conditions, neither *n*-pentylamine nor by-products sometimes observed by others (*13, 19*) have been detected; only very small amounts (less than 1%) of *N*-pentylpiperidine were sometimes observed.

The total HDN activity corresponding to pyridine disappearance at 573 K, measured with a space time of 168 h · g · mol^{-1} depends on the temperature T_R (Fig. 2). After a first initial activity increase, the curve reaches a maximum for T_R = 623 K; after that, the activity progressively decreases to about $T_R \approx 800$ K at which it is roughly 35% of that found at the maximum. By comparing the curves for the two catalytic systems, it appears that nickel has a poor promoting effect, an observation already noted in HDN of pyridine (*20*) or of quinoline (*21*). Moreover, the activity change as a function of T_R is similar with or without presence of the promoter. This is completely different for toluene hydrogenation (*18*): the presence of nickel enhances activity by a factor of ≈10 at low T_R (573 K) whereas the promoting effect is diminished up to ≈2 for high T_R (773 K). Now, the pentane selectivity (S_p) completely depends on both the temperature of pretreatment under H_2 (T_R) and on the presence of the nickel in the catalyst (Fig. 3). At low T_R, for a space time W/F_{pyridine} = 168 g · h · mol^{-1}, selectivity reaches 100% in both cases but, when T_R is increasing, the S_p decrease is much faster with the Ni–Mo system than with the Mo catalyst.

The effects of both T_R and the space time W/F_{pyridine} have been widely explored on the Ni–MoS_2/γ-Al_2O_3 catalyst (Fig. 4a and 4b). In Fig. 4a the evolution of the pentane selectivity S_P is reported as a function of T_R. For a low space time value (84 h · g · mol^{-1}) the selectivity S_P decreases from about 70 to 40% when T_R increases. On the contrary at higher space times, the pentane selectivity reaches 100% at low T_R and the lower limit is around 45%. Another way

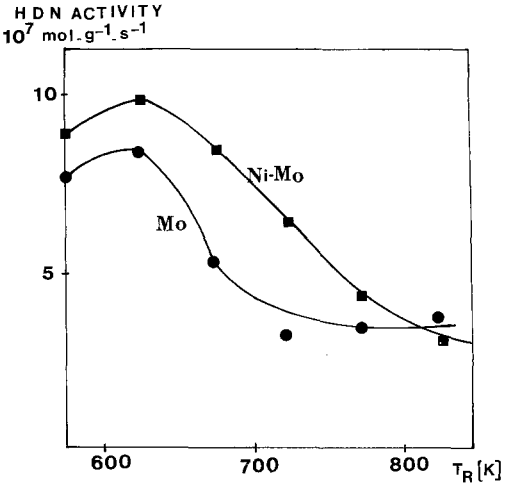

FIG. 2. Pyridine HDN activity versus the pretreatment temperature T_R on Mo/γ-Al_2O_3 and NiMo/γ-Al_2O_3 (W/F_{pyridine} = 168 h · g · mol^{-1}).

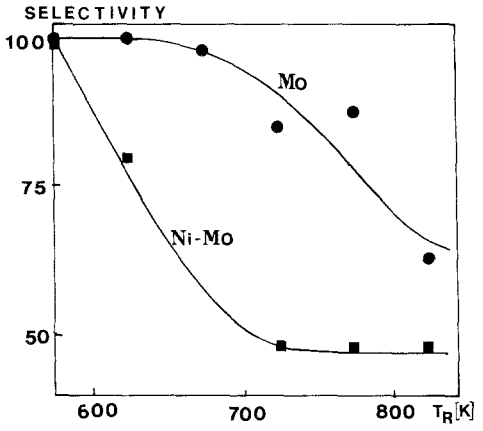

FIG. 3. Selectivity into pentane during pyridine HDN versus the pretreatment temperature T_R on Mo/γ-Al_2O_3 and NiMo/γ-Al_2O_3 ($W/F_{pyridine}$ = 168 h · g · mol^{-1}).

to represent these changes is to plot the pentane selectivity as a function of $W/F_{pyridine}$ for different T_R (Fig. 4b). Although less documented, similar changes have been observed on the Ni–MoS_2/γAl_2O_3 system.

Effect of the H_2 Pressure

The aim of this study was not really to explore the details of the kinetics and determine the orders of the reaction with respect to each compound but to compare the evolution of both hydrogenation and hydrogenolysis reactions under different hydrogen pressures. On the Mo/γ-Al_2O_3 catalyst, the influence of the H_2 pressure on the total pyridine consumption activity and on the product (piperidine, pentane) formation activities has been studied in the 30 to 60-atm P_{H_2} range for two states of the catalyst imposed by T_R at 623 or 773 K. The results are reported in Fig. 5, which represents activities of consumption or production as a function of P_{H_2} (atm) in a log–log scale. Clearly, for T_R = 623 K (Fig. 5a), the H_2 apparent kinetic orders, measured by the slopes of the straight lines obtained, are the same for the total pyridine consumption or piperidine formation rates (≈1.75 to 1.8) and different for the pentane formation rate (≈0.4). For T_R = 773 K (Fig. 5b), the H_2 apparent kinetic orders are close (≈1.5) whatever the activity concerned, even the pentane formation activity. The set of experimental results presented in this paper, in particular the pentane selectivity change as a function of both T_R (Fig. 4b) and $W/F_{pyridine}$ and the kinetic effects of the H_2 pressure which are markedly different for pentane at low T_R on the Mo/γ-Al_2O_3 catalyst (Fig. 5), is indicative that pentane can be produced through two different routes and a detailed analysis on the dual mechanism of pyridine HDN is further discussed in the next section.

The complete set of the H_2 pressure effect for pyridine conversion measurements on the Ni–MoS_2/γ-Al_2O_3 catalyst are reported in Fig. 6. The H_2 apparent orders relative to the pyridine disappearance rate are between 1.50 to 1.70 depending on T_R. Those associated with piperidine formation qualitatively follow the total activity trend with, however, some accidents in the observed straight lines. These evolutions are quite similar to those found on the MoS_2/γ-Al_2O_3 system. More difficult to explain is the dependence on H_2 pressure of the pentane formation rate which on the log–log scale plot (Fig. 6c) does not reveal a linear relationship. The presence of nickel may be associated with this complex H_2 dependence.

DISCUSSION

Pyridine HDN Pathway

The classical pathway for the HDN reaction of pyridine was proposed first by McIlvried (*9*): it mainly consists of two successive steps with an initial reversible formation of piperidine, a hydrogenation product which is desorbed and appears in the gas phase, followed by the hydrogenolysis of the C_{sp_3}–N bond. The quantity of *n*-pentylamine formed at that step is a function of the contact time and is generally small because the second hydrogenolysis step which leads to pentane and ammonia is fast. This reactive scheme has been confirmed several times (*22*) when H_2S was present in the feed.

Within the experimental conditions used in this work, the *n*-pentylamine intermediate has never been detected. For experiments with the catalysts submitted to H_2 at low T_R,

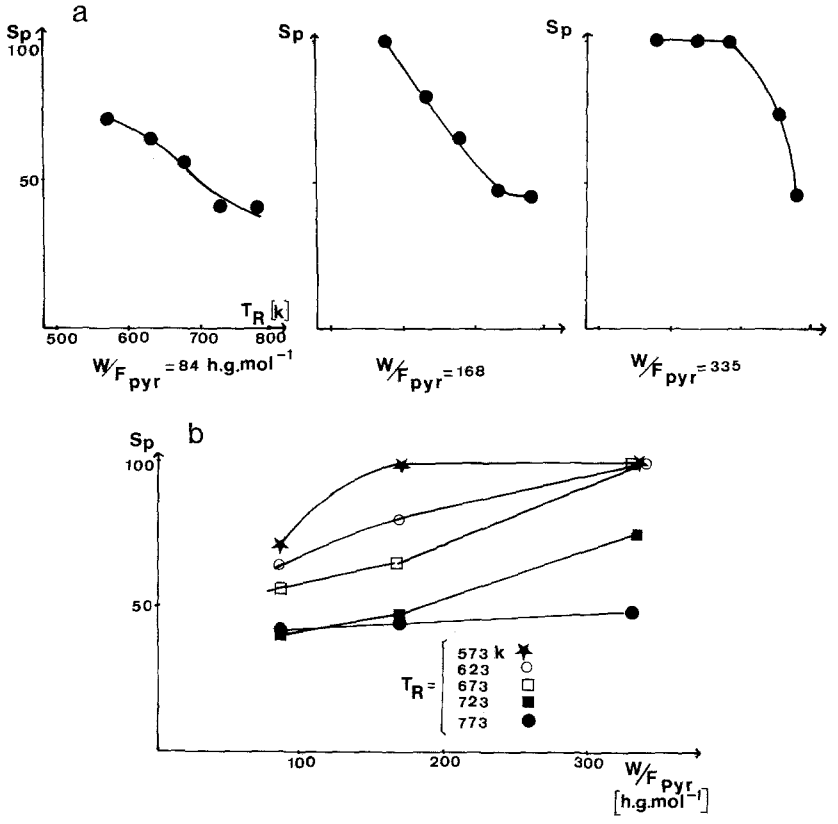

FIG. 4. Selectivity into pentane during pyridine HDN on NiMo/γ-Al_2O_3. (a) versus T_R at various space times, (b) versus space time at various T_R.

the results are in complete agreement with the previous proposed pathway (*9*): indeed, piperidine is considered as a primary product (Fig. 1) and the pentane selectivity is decreasing when the space time $W/F_{pyridine}$ is also decreasing (Fig. 4). Pentane is therefore a secondary product. However, even at low T_R (573–623 K), the initial rate of pentane formation is never equal to zero as shown by the change of the product distribution as a function of the space time (Fig. 1). In addition, for the experiments performed on the catalysts treated at the highest T_R (≈800 K), the pentane selectivity S_P is constant (≈40%) whatever the space time (Fig. 4a or 4b). This implies that the piperidine and pentane formation rates are constant. This evidence is not in agreement with a scheme with successive reactions: the more piperidine is transformed, the more pentane is formed and the selectivity in pentane S_P should increase with the space time as shown for low-T_R-pretreated catalysts. Clearly another possibility of pentane formation is needed to explain these results.

Therefore we propose two alternative mechanisms for HDN of pyridine (Scheme 1):

$$\begin{array}{ccc} \text{PYR} & & \text{PIPE} \\ \downarrow\uparrow & & \downarrow\uparrow \\ \text{PYR}_{(ads)} & \rightleftharpoons & \text{PIPE}_{(ads)} \end{array}$$

$$\rightarrow [n\text{-Pentylamine}_{(ads)}]$$

$$\begin{array}{c} \text{PENT} \\ \downarrow\uparrow \end{array}$$

$$\rightarrow \text{PENT}_{(ads)} + \text{NH}_3 \qquad \text{(A)}$$

$$\begin{array}{ccc} \text{PYR} & & \text{PENT} \\ \downarrow\uparrow & & \downarrow\uparrow \\ \text{PYR}_{(ads)} & \rightarrow & \text{PENT}_{(ads)} + \text{NH}_3 \end{array} \qquad \text{(B)}$$

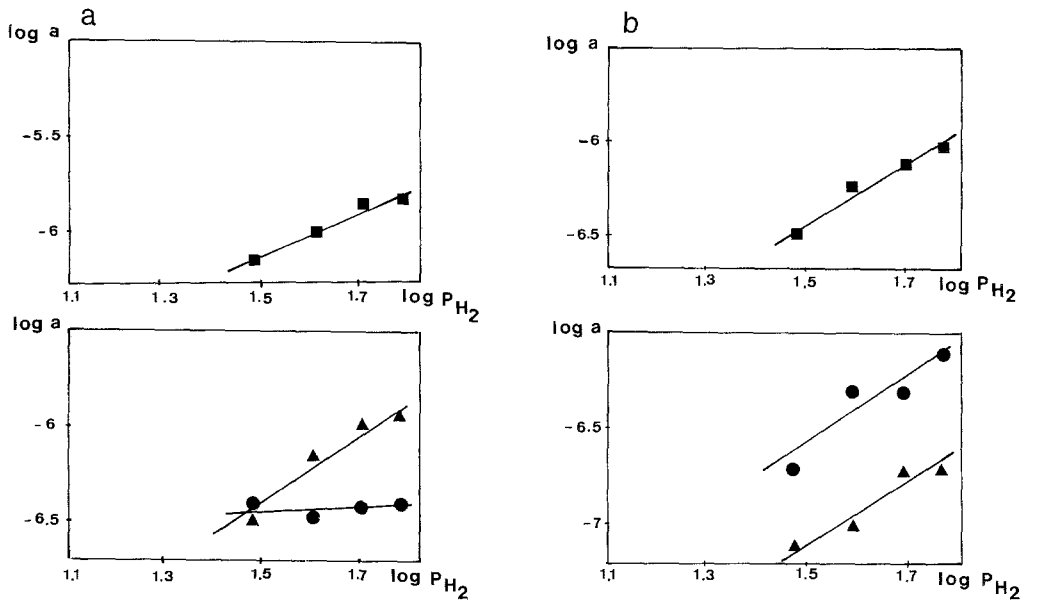

FIG. 5. Pyridine HDN activity, ((■) pyridine conversion, (▲) piperidine production, (●) pentane production), versus P_{H_2} (log–log scale) on Mo/γ-Al_2O_3 ($W/F_{pyridine}$ = 84 h · g · mol^{-1}). (a) T_R = 623 K. (b) T_R = 773 K.

PYR, PIPE, and PENT refer respectively to pyridine, piperidine, and pentane. The subscript (ads) concerns the adsorbed state.

For the catalysts pretreated at low T_R, the pathway A or the McIlvrield (*9*) pathway is preponderant and in agreement with experiments performed with H_2S in the feed, whereas the second route B becomes more and more important when T_R increases. The main experimental evidence for proposing the mechanisms reported in Scheme 1 has been obtained on the Ni–MoS_2 catalyst but some observations like the product distribution (Fig. 1) and the effect of P_{H_2} (Fig. 5) permit one also to ascertain that this dual mechanism is adapted for both catalytic systems. The specific role of nickel is further discussed.

The results obtained at different H_2 pressures are also indicative of the simultaneous existence of two mechanisms for pentane production. In the first scheme, in which an equilibrium between pyridine, hydrogen, and piperidine exists, it is not obvious that the apparent H_2 orders relative to each rate (pyridine consumption or piperidine and pentane production) will be the same. From Figs. 5 and 6, it is clear that, for low T_R, the formation rate of pentane is not as P_{H_2} dependent as the two other rates. For mechanism B, for which piperidine is present as an intermediate adsorbed product but is not detected in the gas phase, the pyridine consumption rate is therefore equal to the formation rate of pentane (the only product, with NH_3). The P_{H_2} effect should be the same in each case. This is observed for high T_R (Fig. 5b) where the apparent H_2 order for pentane formation is the same as that corresponding to pyridine conversion.

Kinetics

By taking into account a large number of already published observations (*8, 9, 22a*) concerning pyridine HDN, it is reasonable to assume the following statements in formulating kinetic relationships:

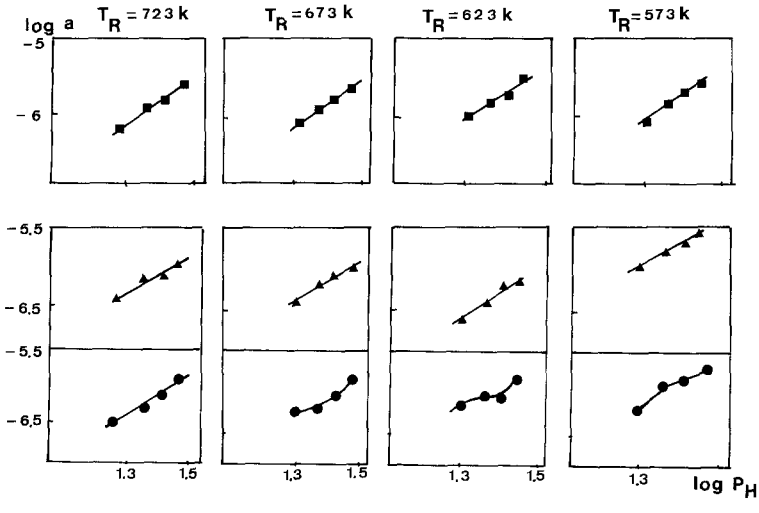

FIG. 6. Pyridine HDN activity ((■) pyridine conversion; (▲) piperidine production; (●) pentane production) versus P_{H_2} (log–log scale) on NiMo/γ-Al_2O_3 catalyst ($W/F_{pyridine}$ = 84 h · g · mol^{-1}) for various T_R.

(i) The adsorption mechanisms of the molecules involved in pyridine HDN are described by a Langmuir–Hinshelwood model.

(ii) There is no competitive adsorption between H_2 and the other molecules. This means that H_2 is adsorbed on sites different from those adsorbing N-containing molecules. In the following the nature of the H-adsorbed species and the apparent kinetic order relative to H_2 are not discussed.

(iii) There is no dissociation in the adsorbed state of the N-containing molecules.

(iv) Adsorption of saturated hydrocarbons (pentane and solvent) are negligible with respect to the N-compounds.

Then rate r_J of a given step J of the HDN process can be written as

$$r_J = k_J \left(\frac{b_{H_2} \cdot p_{H_2}}{1 + b_{H_2} \cdot p_{H_2}} \right) \cdot \frac{b_i \cdot p_i}{1 + \sum_i b_i \cdot p_i}, \quad (1)$$

where b is the adsorption coefficients of the reactants (H_2, pyridine PYR) or products (piperidine PIPE, pentane PENT, and NH_3) and p_i is the partial pressure of compound i.

For the reaction conducted under a constant H_2 pressure, the term in parentheses in Eq. (1) is constant and can be incorporated in an apparent rate constant k'_J.

The objectives of this analysis are to compare the kinetics of the consumption rate of pyridine according the pathways A or B described in Scheme 1. Therefore this rate can be calculated as a function of the pyridine molar fraction $X_{PYR} = p_{PYR}/P^0_{PYR}$:

$$r_1 = \frac{-dX_{PYR}}{dt}, \quad (2)$$

where t(or W/F_{PYR}) represents the space time in h · g · mol^{-1}.

In Table 1 are reported the different kinetic equations we can propose by considering adapted approximations. For mechanism A, two extreme hypotheses have been chosen; the kinetics of pyridine consumption are only influenced by the presence of pyridine and nitrogen products which can have identical (rate r_1^A(a)) or different (rate r_1^A(b)) adsorption coefficients. For mechanism B, piperidine is not detected in the gas phase so that it will not influence the kinetics. Whatever the chosen approximation, only two kinetic equations are obtained

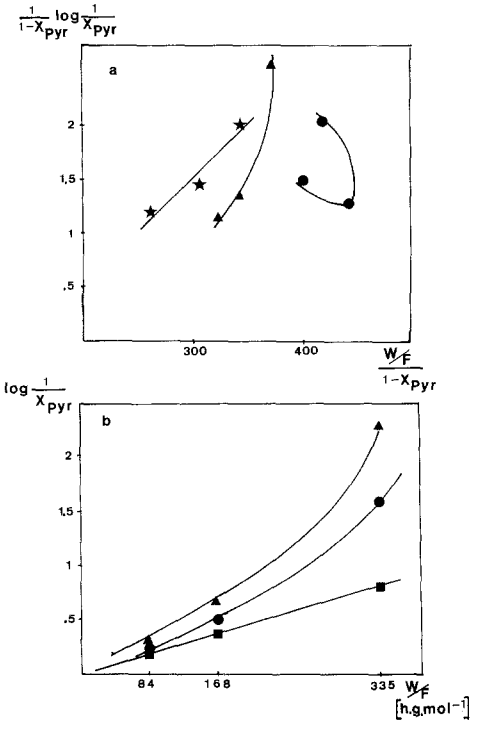

FIG. 7. Plot of: (a) $(1/(1 - X_{PYR}))$ log $(1/X_{PYR})$ as a function of $W/F_{pyridine}/(1 - X_{PYR})$ and of (b) log $(1/X_{PYR})$ as a function of $W/F_{pyridine}$ during pyridine HDN on the NiMo/γ-Al_2O_3 catalyst. (★) T_R = 623 K, (▲) T_R = 673 K, (●) T_R = 723 K, (■) T_R = 773 K.

as r_1^A(a) is identical to r_1^B(b), whereas r_1^A(b) is similar to r_1^B(a). Therefore to test the validity of these equations, Fig. 7 shows both ln $1/X_{PYR}$ as a function of t (actually W/F_{PYR}) and $1/(1 - X_{PYR})$ ln $1/X_{PYR}$ as a function of $t/(1 - X_{PYR})$. Despite the limited number of experimental values, the changes in the curves are clear enough to indicate the trends. For example, for low T_R a linear relationship is obtained with the second representation (Fig. 7a) whereas for higher T_R (T_R = 773 K) the straight line passing through the origin (Fig. 7b) indicates that the first representation is valid. By recalling that at low T_R (typically 623 K), mechanism A is the main route for pyridine conversion, it appears that the best fit corresponds to the rate r_1^A(b). This is in agreement with the analysis of Shih and co-workers (*23*) where it was suggested that only pyridine and nitrogen products are competitively adsorbed on the same sites. Obviously, the basicity and aromatic character of pyridine are different from those of piperidine and ammonia, and therefore it is inferred that $b_{NP} \neq b_{PYR}$ (NP, nitrogenated products). The extrapolation of the obtained straight line (Fig. 7a) to a zero value of $t/(1 - X_{PYR})$ gives a negative value which means, considering the integrated relationships reported in Table 1 that b_{PYR} is higher than b_{NP}, as expected. At high T_R mechanism B becomes more important and in that case the best fit corresponds to $b_{PYR} = b_{NH3}$. This approximation is not contradictory with the previous one as the pyridine conversion route is different, which implies that, even in the adsorption step, pyridine is differently adsorbed. The main benefit of this kinetic analysis is therefore to show that the dual mechanism for pyridine conversion is mainly due to a different adsorption mechanism on the sites present on the catalysts studied. In fact, the steps are always the same and the hydrogenation reaction remains a prerequisite but at high reduction temperatures T_R, it is probable that the active sites do not allow the piperidine desorption either because its adsorption is too strong or because the hydrogenolysis step is too fast.

Nature of Adsorption Sites: Role of Nickel

We point out here that the effect of T_R on the catalysts we have investigated is to remove sulfur progressively at the edges of the supported MoS_2 platelets. Therefore the nature of the active sites is changing upon progressive increase of T_R and it is not so surprising that a different HDN mechanism takes place for low and high T_R. At low T_R, the number of sulfur vacancies is relatively small and the pathway relevant to the MacIlvried network (*9*) has been found to be dominant. This is consistent with the fact that HDN is normally performed with a given

TABLE 1

Determination of the Pyridine Consumption Rates According to the Pathways A or B Proposed in Scheme 1

Approximations	Rate of pyridine consumption	Integrated relationships
Mechanism A		
$P^0_{PYR} = p_{PYR} + p_{PIPE} + p_{NH_3}$		
(a) $b_{PYR} \cong b_{PIPE} \overset{b}{\cong} b_{NH_3}$	$r_1^A(a) = \dfrac{k_1' \cdot b_{PYR} \cdot P^0_{PYR} \cdot X_{PYR}}{1 + b_{PYR} \cdot P^0_{PYR}}$	$\ln \dfrac{1}{X_{PYR}} = \dfrac{k_1' \cdot b_{PYR} \cdot P^0_{PYR}}{1 + b_{PYR} P^0_{PYR}} \cdot t$
(b) $b_{NP} \neq b_{PYR}$	$r_1^A(b) = \dfrac{k_1' \cdot b_{PYR} \cdot P^0_{PYR} \cdot X_{PYR}}{1 + b_{PYR} \cdot X_{PYR} \cdot P^0_{PYR} + b_{NP}(1 - X) P^0_{PYR}}$	$\dfrac{1}{1 - X_{PYR}} \cdot \ln \dfrac{1}{X_{PYR}} = \dfrac{k_1' \cdot b_{PYR} \cdot P^0_{PYR}}{1 + b_{NP} \cdot P^0_{PYR}} \cdot \dfrac{t}{1 - X_{PYR}} - \dfrac{(b_{PYR} - b_{NP}) P^0_{PYR}}{1 + b_{NP} \cdot P^0_{PYR}}$
Mechanism B		
$P^0_{PYR} = p_{PYR} + p_{NH_3}$ as PIPE is not detected in the gas phase		
(a) $b_{PYR} \neq b_{NH_3}$	$r_1^B(a) = \dfrac{k_1' \cdot b_{PYR} \cdot P^0_{PYR} \cdot X_{PYR}}{1 + b_{PYR} \cdot P^0_{PYR} \cdot X_{PYR} + b_{NH_3}(1 - X_{PYR}) \cdot P^0_{PYR}}$	$\dfrac{1}{1 - X_{PYR}} \cdot \ln \dfrac{1}{X_{PYR}} = \dfrac{k_1' \cdot b_{PYR} \cdot P^0_{PYR}}{1 + b_{NH_3} \cdot P^0_{PYR}} \cdot \dfrac{t}{(1 - X_{PYR})} - \dfrac{(b_{PYR} - b_{NH_3}) \cdot P^0_{PYR}}{1 + b_{NH_3} \cdot P^0_{PYR}}$
(b) $b_{PYR} \cong b_{NH_3}$	$r_1^B(b) = \dfrac{k_1' \cdot b_{PYR} \cdot P^0_{PYR} \cdot X_{PYR}}{1 + b_{PYR} \cdot P^0_{PYR}}$	$\ln \dfrac{1}{X_{PYR}} = \dfrac{k_1' \cdot b_{PYR} \cdot P^0_{PYR}}{1 + b_{PYR} \cdot P^0_{PYR}} \cdot t$

Note. NP, nitrogenated products; k_1' = apparent rate constant of step 1.

partial pressure of H_2S which probably imposes the S/Mo stoichiometry and limits the number of anionic vacancies.

The role of nickel in this investigation is rather complex since it can be considered also as a catalytic site because the treatment under H_2 at T_R may remove S bound to nickel or nickel can influence the properties of the sites associated with molybdenum; the extent of the nickel influence does not appear very important in terms of pyridine HDN as a function of T_R (Fig. 2): for low T_R, the Ni–MoS_2 activity is slightly higher than the Mo activity and Ni is therefore considered as a weak promoter for HDN. At the highest T_R, both systems have comparable activity and in that case, nickel is no longer considered a promoter. The more detectable influence of nickel in this series of experiments concerns the pentane selectivity S_P (Fig. 3): the evolution, starting from the same value (S_P = 100%) is quite different for the MoS_2 and Ni–MoS_2 systems when T_R increases. Taking into account that two HDN mechanisms exist simultaneously for pyridine transformation, nickel may favor route B more rapidly when T_R increases.

CONCLUSION

The mechanism for HDN of pyridine on MoS_2 and Ni–MoS_2/γ-Al_2O_3 catalysts has been found to be dependent on the temperature of treatment under H_2 (T_R) carried out before the catalytic tests. The effect of T_R is to progressively remove sulfur at the edges of the supported MoS_2 phase and create coordinatively unsaturated Mo sites. For low T_R, a reaction network similar to that already described by McIlvried (*9*) has been found to be the main pyridine conversion route whereas a second mechanism for which no piperidine desorption occurs has been evidenced for high T_R. From kinetic arguments, it has been deduced that the mode of pyridine adsorption is different for these two mechanisms. The way in which the experiments are conducted (absence of H_2S in the feed during the HDN tests) may lead one to suppose that the catalyst is irreversibly evolving during the tests conducted under high H_2 pressure. We have checked (*18*) the total reversibility of the HDN results as resulfidation after a H_2 treatment at T_R = 773 K restores the original activity of the catalyst.

The question arises as to whether, under practical conditions where H_2S and/or sulfur compounds are present in the feed, the second pathway we have indicated still exists. No definite answer can be given but what is clear from this study is the fact that the mode of adsorption of molecules (i.e., nitrogenated compounds), and consequently their reactivity, is influenced by the nature of the active site for which the number of coordinative unsaturations is in dynamic evolution as a function of the H_2S partial pressure.

REFERENCES

1. Zdražil, M., *Appl. Catal.* **4,** 107 (1982).
2. Vrinat M., *in* "Surface Properties and Catalysis by Non-Metals" (J. P. Bonnelle, B. Delmon, and E. Derouane, Eds.), p. 391. Reidel, Dordrecht, 1983; Vrinat M., *Appl. Catal.* **6,** 137 (1983).
3. Le Page, J. F., "Catalyse de Contact," p. 441. Technip, Paris, 1978.
4. Katzer, J. R., and Sivasubramanian, R., *Catal. Rev. Sci. Eng.* **20,** 635 (1979).
5. Schulz, H., Schon, M., and Rahman, N. M., *in* "Catalytic Hydrogenation, A Modern Approach" (L. Červeny, Ed.), Studies in Surface Science and Catalysis, Vol. 27, p. 204. Elsevier, Amsterdam, 1986.
6. Ho, T., *Catal. Rev. Sci. Eng.* **30,** 117 (1988).
7. Satterfield, C. N., Modell, M., and Mayer, J. F., *AIChE J.* **21,** 1100 (1975).
8. Satterfield, C. N., and Coccheto, J. F., *AIChE J.* **21,** 1107 (1975).
9. McIlvried, M. G., *Ind. Eng. Chem. Process Des. Dev.* **10,** 125 (1971).
10. Moreau, C., Aubert, C., Durand, R., Zmimita, N., and Geneste, P., *Catal. Today* **4,** 117 (1988).
11. Laine, R-M., *Catal. Rev. Sci. Eng.* **25,** 459 (1983); *New J. Chem.* **11,** 543 (1987).
12. Ledoux, M. J., Puges, P. E., and Maire, G., *J. Catal.* **76,** 285 (1982); Ledoux, M. J., and Sedrati, M., *J. Catal.* **83,** 229 (1983); Ledoux, M. J., *Appl. Catal.* **9,** 31 (1984).
13. Sonnemans, J., van den Berg, G. H., and Mars, P., *J. Catal.* **31,** 220 (1973). Sonnemans, J., Neyens, W. J., and Mars, P., *J. Catal.* **34,** 230 (1974).
14. Satterfield, C. N., and Gültekin, S., *Ind. Eng. Chem. Process. Des. Dev.* **20,** 62 (1981).

15. La Vopa, V., and Satterfield, C. N., *J. Catal.* **110,** 375 (1988).
16. Kasztelan, S., Jalowiecki, L., Wambeke, A., Grimblot, J., and Bonnelle, J. P., *Bull. Soc. Chim. Belg.* **96,** 1003 (1987).
17. Wambeke, A., Jalowiecki, L., Kasztelan, S., Grimblot, J., and Bonnelle, J. P., *J. Catal.* **109,** 320 (1988).
18. Bonnelle, J. P., Wambeke, A., Kherbeche, A., Hubaut, R., Jalowiecki, L., Kasztelan, S., and Grimblot, J., *in* "Advances in Hydrotreating Catalysts" (M. L. Occelli and R. G. Anthony, Eds.), p. 123. Elsevier, Amsterdam, 1989.
19. Nelson, N., and Levy, R. B., *J. Catal.* **58,** 485 (1979).
20. Ledoux, M. J., Agostini, G., Benazour, R., and Michaux, O., *Bull. Soc. Chim. Belg.* **93,** 635 (1984).
21. Perot, G., Brunet, S., and Hamzé, N., *in* "Proceedings, 9th International Congress on Catalysis, Calgary, 1988" (M. J. Phillips and M. Ternan, Eds.), Vol. 1, p. 19. Chem. Institute of Canada, Ottawa, 1988.
22. (a) Descat, G., Bachelier, J., Duchet, J. C., and Cornet, D., *in* "Proceedings, IXth Iberoamerican Symposium on Catalysis, Lisbon," Vol. 2, p. 1284, 1984; (b) Satterfield, C. N., Modell, M., and Wilkens, J. A., *Ind. Eng. Chem. Process Des. Dev.* **19,** 154 (1980); (c) Ho, T. C., Montagna, A. A., and Steger, J. J., *in* "Proceedings, 8th International Congress on Catalysis, Berlin, 1984," Vol. 2, p. 257. Dechema, Frankfurt-am-Main, 1984.
23. Shih, S. S., Katzer, J. R., Kwart, H., and Stiles, A. R., *Prepr. Pap.-Am. Chem. Soc., Div. Petrol. Chem.,* 919 (1977).